Land Cover Classification and Change Analysis in the North of England

1. Introduction

Remote sensing is a powerful tool that enables the study of the Earth's surface and its processes from a distance, using data acquired by sensors on satellites, aircrafts, or drones. Launched in 1972, the United States Government developed and operated the Landsat satellite program which has collected over 9 million images of the Earth's surface. The program has been instrumental in advancing the field of remote sensing and has contributed to numerous scientific studies (Williams, et al., 2006).

Land Cover Classification (LCC) is an important aspect of remote sensing and involves the identification and mapping of different types of land, such as forests, crops, water bodies, and urban areas. LCC is crucial for a wide range of applications, from land management to environmental and atmospheric monitoring. Remote sensing provides a cost-effective and efficient means of obtaining large-scale and up-to-date information about land cover, which can be used to support decision-making processes at local, regional, and global scales (Fichera, et al., 2012). In recent years, advances in remote sensing technology, including improved sensors, processing algorithms, and cloud computing, have greatly enhanced the accuracy and resolution of LCCs (Phalke, et al., 2020).

On behalf of a Wildlife National Governing Body (WNGB), this investigation seeks to explore the fundamental concepts of remote sensing, undertaking a supervised LCC of two Landsat 5 satellite images. Focusing on woodland, with some species of woodland birds rapidly declining, this research will develop a greater understanding of environmental change to assess the conservation of natural woodland habitats (RSPB, 2017).

2. Methodology

i. Study Area

The study focused on the North of England, specifically Landsat Path: 203 and Row: 22. The area captures major urban areas such as Leeds, Newcastle, and Hull as well as National Parks and Areas of Outstanding Natural Beauty including the Pennines, North York Moors and Yorkshire Dales.

ii. Software, Data Acquisition and Preparation

TerrSet was utilised throughout the study. TerrSet is a geospatial software platform for monitoring and modelling Earth systems, integrating tools for remote sensing, and spatial analysis (TerrSet, 2016). This study utilises imagery from the Landsat 5 Satellite, which was in operation from 1984 until 2013. Carrying a Thematic Mapper (TM) sensor, it captured images of the Earth's surface in multiple spectral bands, ranging from visible to thermal infrared (Figure 1). The images have a spatial resolution of 30m per pixel and a typical Landsat 5 scene covers an area of approximately 31,100km^2. Each pixel for every spectral band has a brightness integer value between 0-255.

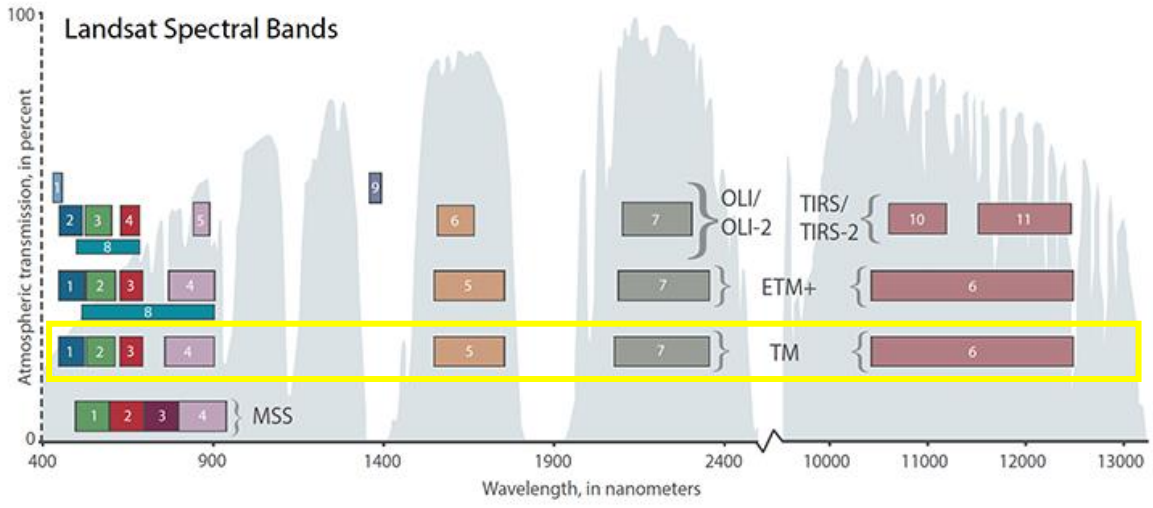

Figure 1: Graphic showing the evolution of Landsat's spectral bands, including Landsat 5 TM (highlighted yellow). Adopted from NASA (Rocchio & Barsi, 2016).

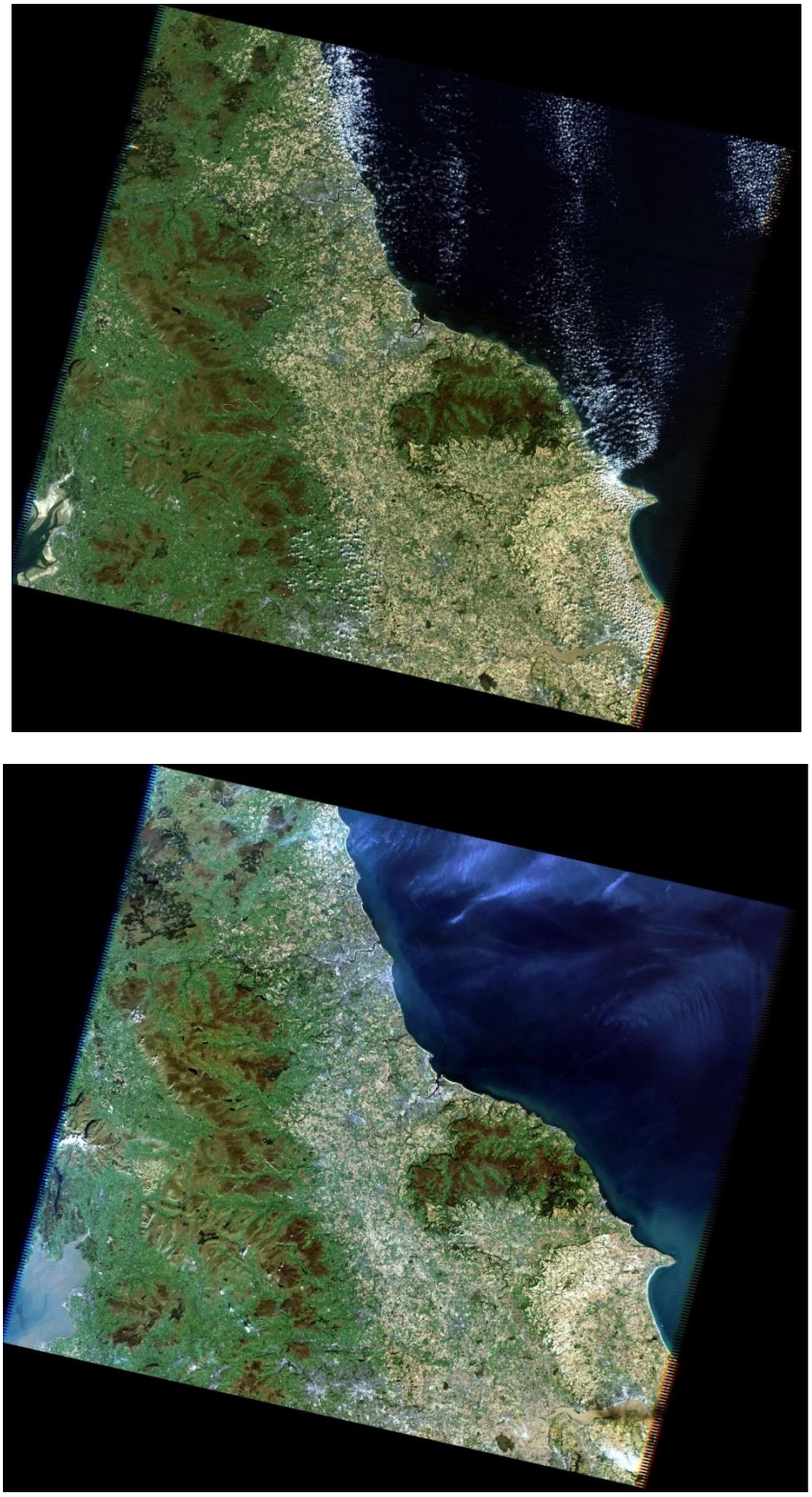

Figure 2: Landsat 5 scenes from 08/09/2004 (top) and 28/09/2011 (bottom). True colour images, produced by applying the red, green, and blue colour guns to the bands 3, 2, and 1 respectively, comparable to what is visible with the human eye. Created using Terrset.

Landsat images were downloaded from the U.S. Geological Survey Earth Explorer website (USGS, 2023). When searching, a cloud cover range was set to 0% - 10%. The best months for remote sensing classification can vary depending on the specific land cover being studied. In general, the months of May to September tend to be the best for remote sensing in the UK (Ioannis & Meliadis, 2011). These months are characterised by lower cloud cover and vegetation is most distinguishable reducing the chance of misclassification. Drawing on the rational describe above, the two images that form the basis of this analysis were from 08/09/2004 and 28/09/2011 (Figure 2).

iii. Land Cover Classification (LCC)

LCC using satellite imagery is the process of grouping pixels into classes based on their spectral signature (Karlsson, 2003). This can be achieved through several techniques, primarily using automated computer technologies. These automated methods can be further divided into two groups: 1) supervised classification, 2) unsupervised classification (Abburu & Golla, 2015). This analysis uses a supervised classification, which is the most frequently applied method for quantitative analyses of remote sensing imagery (Richards & Jia, 2006). The LCC, in accordance with the WNGO's objectives, aims to classify land into the following six classes:

1. Water
2. Agriculture
3. Grassland
4. Woodland
5. Artificial Surface
6. Cloud

The LCC was implemented following the method outlined in Table 1:

Step:	Method:

1. Defining LCC classes and training sites	• Once LCC classes were defined, training sites were selected based on true and false colour composite Landsat imagery and high-resolution Google Earth imagery.
	• The near-infrared reflectance spectrum is a highly effective method for distinguishing healthy vegetation. Replacing the visible red (band 3) with the near-infrared (band 4) creates a false colour composite image, healthy vegetation appears red whilst urban areas appear cyan blue. Healthy plants reflect a greater amount of energy in the near-infrared spectrum, while water tends to absorb it (Jensen, 2015). False colour composite imagery was useful for deciphering training sites for agriculture, grassland and woodland.
	• When defining training sites, there should be a satisfactory sample of pixels for each cover type for the classification to be statistically adequate.
	  ○ The TerrSet manual suggests a minimum of 10 times as many pixels per training class as there are bands in the images being classified, whilst ESRI documentation recommends the number of pixels per training area should be between 10n and 100n, where n represents the number of bands in the imagery (ESRI, 2011; TerrSet, 2016).
	  ○ Generally, it is advisable to include more pixels in each training class, within a limit, and to have several training sites for each class (NASA, 2017).
	  ○ Conversely, creating excessively large training sites, such as including a significant portion of the ocean area in one large training site, can result in bias during the automated classification. To prevent this, it is suggested that training sites occupy no more than 5% of a land cover class (UBC, 2018).
	• Although training sites are ideally spectrally homogenous, it is important to capture an array of spectral signatures associated with each land cover type (UBC, 2018). If only one training site for each class is chosen, then it is unlikely all the spectral variability will be captured. Creating several training sites for each class located in different parts of the scene is suggested (NASA, 2017).
	• Based on the previous research detailed above, this analysis delineates the digitisation of at least 5 distinct polygons across the scene for each class.

2. Signature Extraction	• The goal of training is to accumulate a variety of spectral signatures associated with each LCC class (NASA, 2017). Once defined, signatures were extracted for each LCC class. • Signature files were developed in TerrSet using the MAKESIG tool. • Statistical plots, such as histograms, line and scatter plots are useful ways to display the numerical content of a Landsat band and the spectral signatures of selected training sites (Papp, 2018). If statistical plots do not show distinct differences in the spectral response patterns of the training sites, it may be challenging to classify unknown pixels correctly during image classification. Consequently, the quality of the final output heavily depends on the creation of reliable training sites and careful examination of the statistical results (UBC, 2018). ○ Effective training sites should display a single peak in histograms and have distinctive statistical properties. Erroneous misclassifications may arise if; the scatterplot of a training area displays multiple clusters, or the histogram has multiple peaks, or the statistical properties of an area show significant overlap (ESRI, 2011). • This analysis utilised statistical plots to check the validity of the spectral signatures and training site selection went through several iterations. Changes were made as necessary to ensure adequate signatures.
3. Image Classification	• Once satisfactory signature files were created, an image classification was undertaken to assign the remaining unknown unclassified pixels to one of the known classes, based on the pixel's reflectance values (UBC, 2018). • This analysis uses a hard classification due to its robustness and computational efficiency when working with large datasets (Jensen, 2015). • Two of the more commonly used algorithms are Minimum Distance and Maximum Likelihood (UBC, 2018). • The most appropriate algorithm depends on various factors such as the type and quality of the data, the complexity of the study area, and the number and variability of the LCC classes. • Although there is a wide range of image classification algorithms, one will not consistently provide the best classification (UBC, 2018). • Since training sites were well-defined, the Maximum Likelihood algorithm was chosen as it often yields the best results, allowing for better discrimination between land cover classes. Notably, in cases where training sites are not clearly defined, the Minimum Distance algorithm with standardised distances often performs better (TerrSet, 2016).

Table 1: Land Cover Classification Methodology.

iv. Accuracy Assessment

Completing an accuracy assessment of the results with ground truth data is the final and arguably most crucial part of the LCC process (Rwanga & Ndambuki, 2017). Typically, ground truth data is collected in the field or using high-resolution imagery. To avoid extensive ground surveys, this study utilised Google Earth's archive satellite imagery and Google Street View to locate ground truth points, ensuring the imagery was from the same year as the Landsat imagery under investigation. This saved considerable time and ensured evenly distributed validation points across the scene (Lillesand, et al., 2015). Sampling aims to collect an unbiased selection of the total population (Jensen, 2015). Although there are numerous sample techniques including random, stratified, and clustered, this analysis employs a judgmental sampling approach whereby locations are intentionally selected for inclusion based on expert knowledge and judgment.

Validation points were added in the form of a vector file. To avoid bias, a sample of pixels independent of those developed to train the classification were used (Strahler, et al., 2006). A simple values file was created to record the true landcover class at each location. The values file was used in combination with the vector file to produce a raster image showing the true classes found at the validation point locations. By comparing this raster image to the classified map using TerrSet's ERRMAT tool, errors of omission, errors of commission, and the overall proportional error were tabulated (TerrSet, 2016).

Fitzpatrick-Lins suggests that a suitable sample size for an accuracy assessment can be calculated using the formula for the binomial probability theory (Fitzpatrick-Lins, 1981). The formula is as follows:

$$N = \frac{Z^2 * p * (1 - p)}{d^2}$$

where:

- N is the number of validation points required.
- Z is the standard normal deviation for the desired confidence level (e.g. Z = 1.96 for a 95% confidence level).
- p is the estimated proportion of the study area covered by the land cover class of interest.
- d is the desired accuracy level, expressed as a proportion of the study area (e.g. 0.05 for 5% accuracy).

$$N = \frac{1.96^2 * 0.05 * (1 - 0.05)}{0.05^2}$$

$$N = 72.9$$

Based on Fitzpatrick-Lins' suggested requirements, estimating woodland makes up 5% of the LCC, validating with 95% confidence and 5% accuracy, this analysis used a total of 60 ground reference points, 10 per class.

TerrSet's ERRMAT tool generates an error matrix whereby the diagonal tabulations indicate cases where the mapped category corresponds to the true value. Errors of omission are proportional errors along the bottom of the graph, while Errors of Commission are along the right-hand edge. Errors of omission represent situations where sample points of a specific category were mapped as something different, while Errors of commission involve cases where locations mapped as a particular category were something else in reality (TerrSet, 2016).

A thorough analysis of this information enabled the evaluation of the amount of error, its location, and possible rectification (TerrSet, 2016). Additionally, accessing the accuracy of individual parameters is useful to evaluate the model's performance in respect of a particular LCC class of specific interest, such as woodland (Rwanga & Ndambuki, 2017).

In addition to the error matrix, the ERRMAT details the Conditional (Kappa) Coefficient of Agreement, a statistical measure used to assess the accuracy of the image classification by comparing the observed classification results with the expected results based on chance. It considers both the overall accuracy of the classification and the degree of agreement beyond chance and is particularly useful when using fewer LCC classes (Jensen, 2015).

The Kappa value ranges from -1 to 1. Values closer to 1 indicate higher levels of agreement between the observed and expected classifications, values closer to 0 indicate no better agreement than chance, and values closer to -1 indicate less agreement than chance (Table 2). A negative value implies the classification is worse than random guessing (Rwanga & Ndambuki, 2017).

Kappa Statistic	Strength of Agreement
<0.00	Poor
0.00 - 0.20	Slight
0.21 - 0.40	Fair
0.41 - 0.60	Moderate
0.61 - 0.80	Substantial
0.81 - 1.00	Almost Perfect

Table 2: Categorisation of the Kappa Statistic, adopted from (Rwanga & Ndambuki, 2017).

v. Change Analysis

Land Change Modeller (LCM) within TerrSet provided a comprehensive set of tools for analysing land cover change between 2004 and 2011. Prior to analysis, the RESAMPLE tool was utilised to spatially align the two Landsat images and mask layers were applied to remove any obvious misclassified pixels on the image margins. The LCC outputs were also manipulated in QGIS and scrutinised by several geoprocessing tools, such as 'Raster Unique Values Report'.

3. Results

i. False Colour Composite

False colour composites of both images clearly reveal the locations of healthy vegetation such as woodland and grassland, in comparison to urban areas and degraded agricultural land (Figure 3). Morecambe Bay is a notable feature with differing tidal levels visible In the Southwest corner of the scenes. Although cloud cover appeared greater in 2004, high altitude cirrus clouds are evident in the 2011 scene.

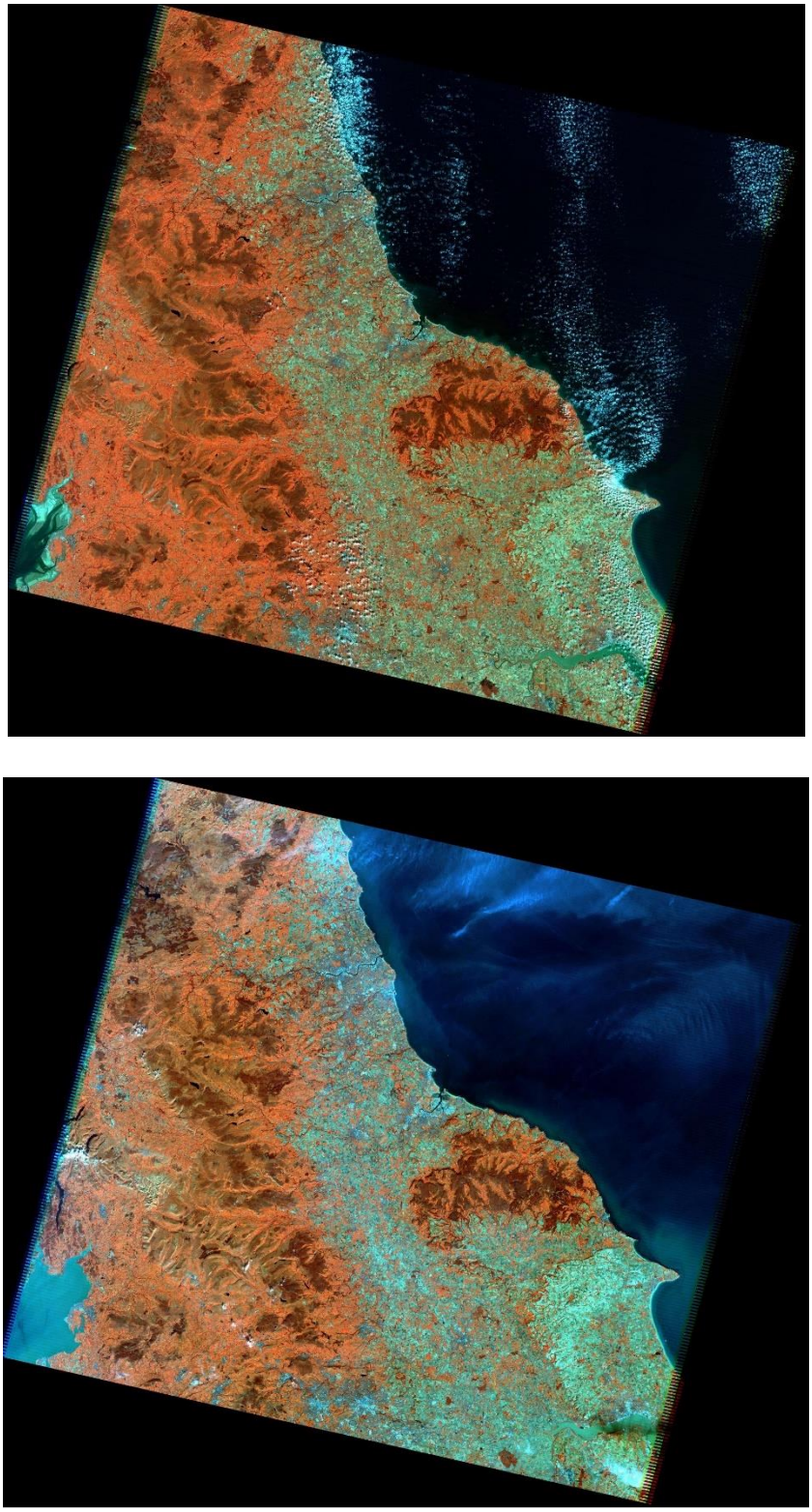

Figure 3: Landsat 5 false colour images from 08/09/2004 (top) and 28/09/2011 (bottom). Created using Terrset by applying the red, green and blue colour guns to the bands 4, 2 and 1, respectively.

ii. Spectral Signatures

Statistical plots display the water and cloud classes have the most distinct spectral signatures across the 7 bands (Figure 4). Artificial surfaces and clouds have the most variation in reflectance values due to the variety of surfaces included within their respective training sites. There is a large degree of overlap between agricultural land and grassland. Little separability between signatures is a source of spectral confusion between cover types and could result in misclassification. Importantly woodland has a relatively distinct spectral signature.

Figure 4: Signature composition charts displaying mean values for each spectral band and land cover class from 08/09/2004 (top) and 28/09/2011 (bottom). Derived from the training site data, the y-axis represents the mean reflectance value, and the x-axis represents the spectral band. Created using Terrset.

iii. Land Classification and Change Analysis

The land classification appears precise, with the vast majority of pixels belonging to the most suitable land cover type. Agriculture and water are the dominant land cover types making up a combined land cover of 69% and 73% in 2004 (Table 3, Figure 5) and 2011 (Table 4, Figure 6) respectively.

Misclassification is evident in some areas. For example, the 2004 scene was captured at low tide and large areas around Morecambe Bay were classified as artificial surfaces. Desktop research reveals those areas were sand and mud, not artificial surfaces (Figure 7). Additionally, artificial surfaces were classified as more prominent in 2004. However, this is likely not a true reflection of reality but rather a result of misclassification. Moreover, the classification struggled to classify some cloud coverage correctly. In some instances, pixels located at the fringes of cloud cover have been assigned as artificial surfaces due to similarities in spectral signature. The classification also struggled with cloud

shadows, again resulting in instances of misclassification. Consequently, the higher coverage of artificial surfaces in 2004 compared to 2011 can partly be attributed to higher cloud cover.

This analysis indicates woodland coverage has increased between 2004 and 2011 (Figure 8, Figure 10). This is important for bird species that rely on a woodland habitat. The results reflect previous research that reports land area covered by woodland has increased from 9% to 13.3% between 1980 and 2022 (ONS, 2022). Land cover analysis indicates that grassland is the main contributor to the net gain in woodland increase. However, an 8km^2 contribution of woodland has come from water (Figure 9). Although possible, this is unlikely. Desktop research revealed some coastal shallow water and bedrock were misclassified as woodland.

Although some land cover classes, such as water and artificial surfaces will not have a major effect on woodland prominent bird species, it is important to consider all LCC classes to assess the validity of the classification.

Land Cover Class	Area (km^2)	Percentage (%)
Water	9593	29
Agriculture	12989	40
Grassland	5456	17
Woodland	799	2
Artificial Surface	2914	9
Cloud	792	2

Table 3: Area and percentage for each land cover class based on the 2004 image classification. Created using QGIS and Excel.

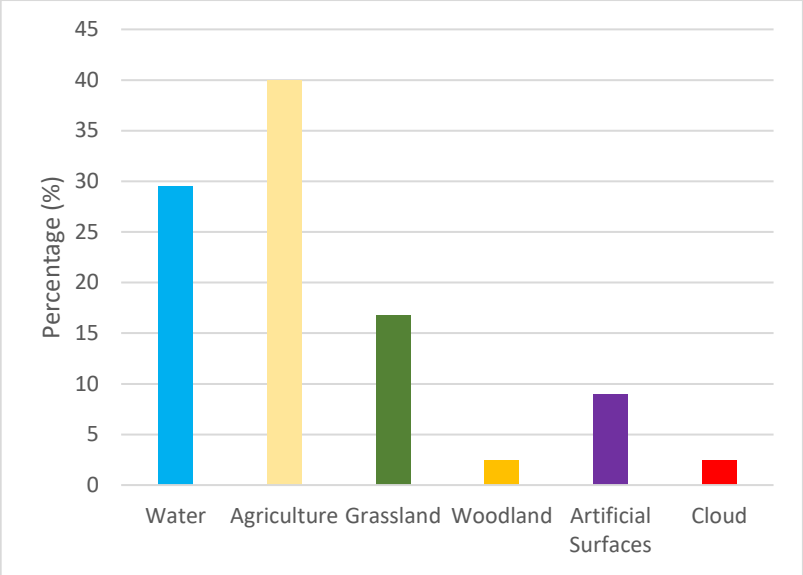

Figure 5: Bar chart displaying percentage allocations for each land cover class based on the 2004 image classification. Created using Excel.

Land Cover Class	Area (km^2)	Percentage (%)
Water	10273	32
Agriculture	13419	41
Grassland	5593	17
Woodland	871	3
Artificial Surface	2165	7
Cloud	222	1

Table 4: Area and percentage for each land cover class based on the 2011 image classification. Created using QGIS and Excel.

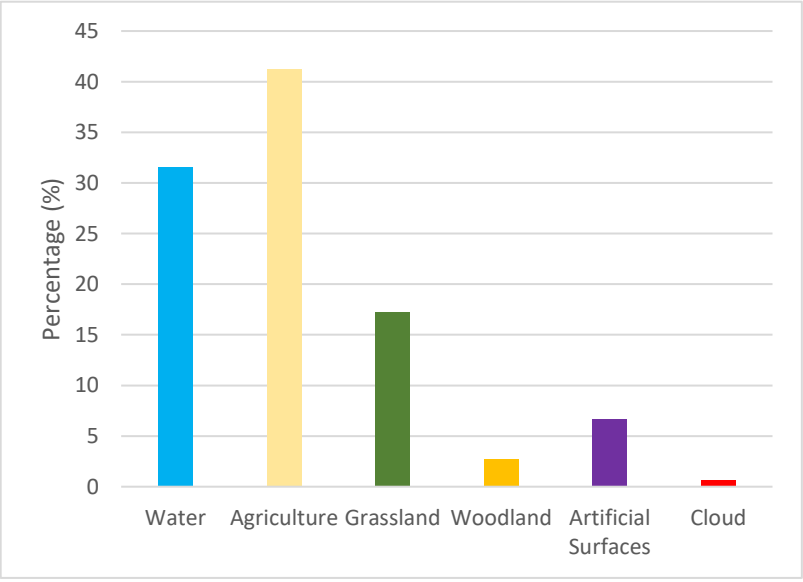

Figure 6: Bar chart displaying percentage allocations for each land cover class based on the 2011 image classification. Created using Excel.

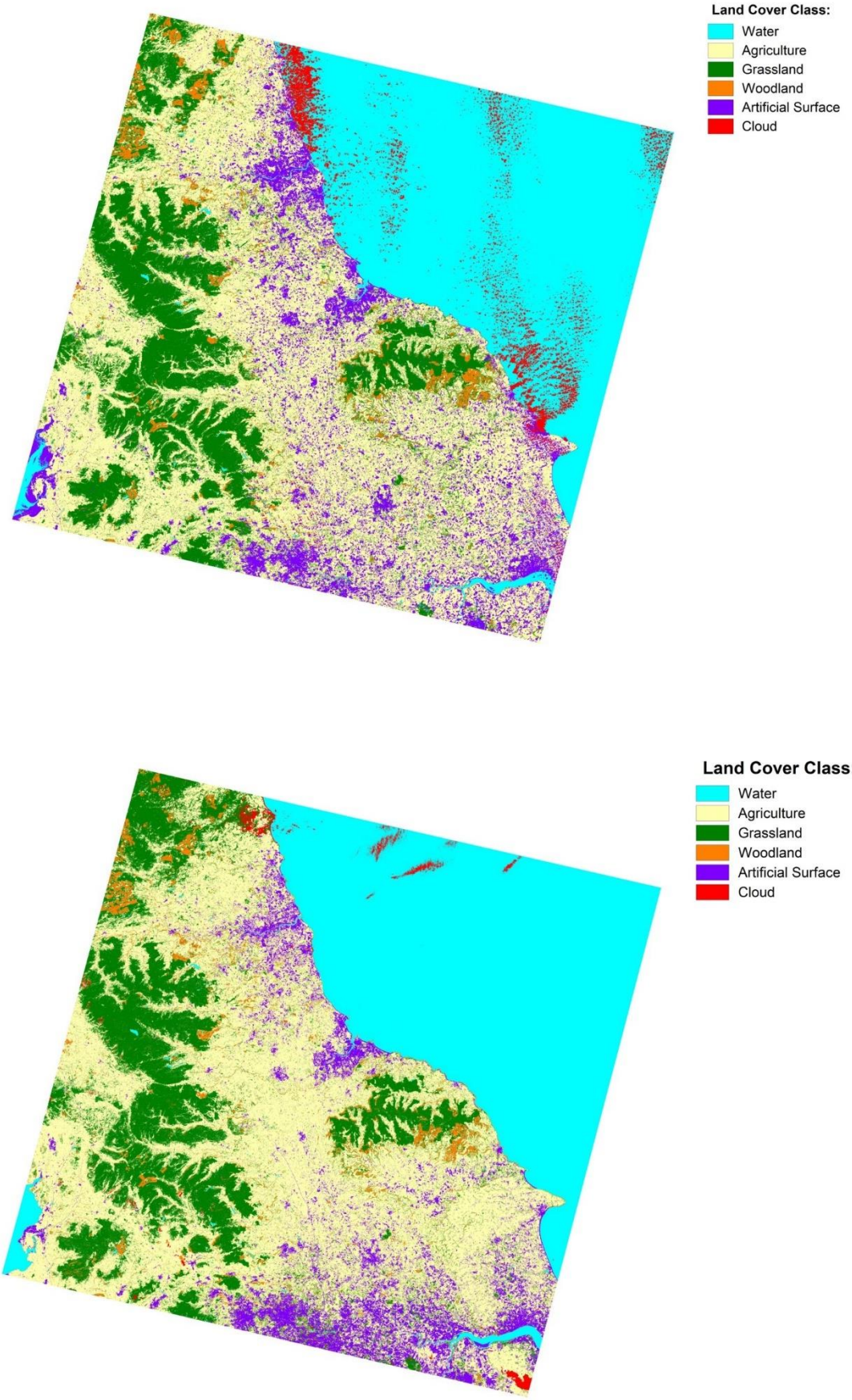

Figure 7: Land classification outputs from 08/09/2004 (top) and 28/09/2011. Created using Terrset.

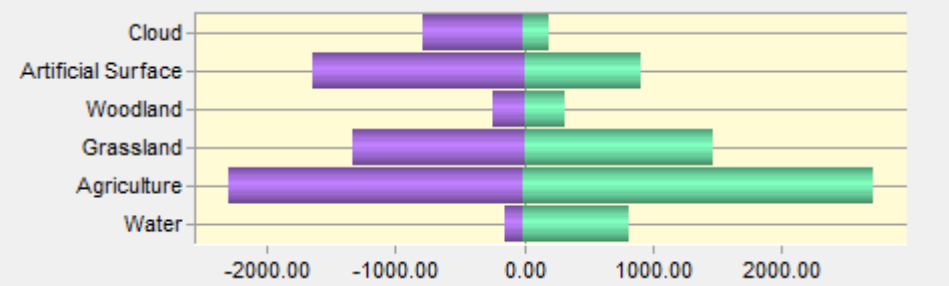

Figure 8: Gains and losses (km²) from all land cover classes between 2004 and 2011. Created using Terrset.

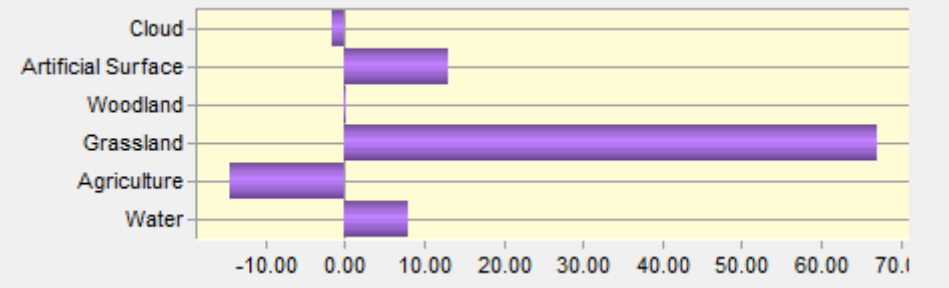

Figure 9: Contributions (km²) to the net change in woodland between 2004 and 2011. Created using Terrset.

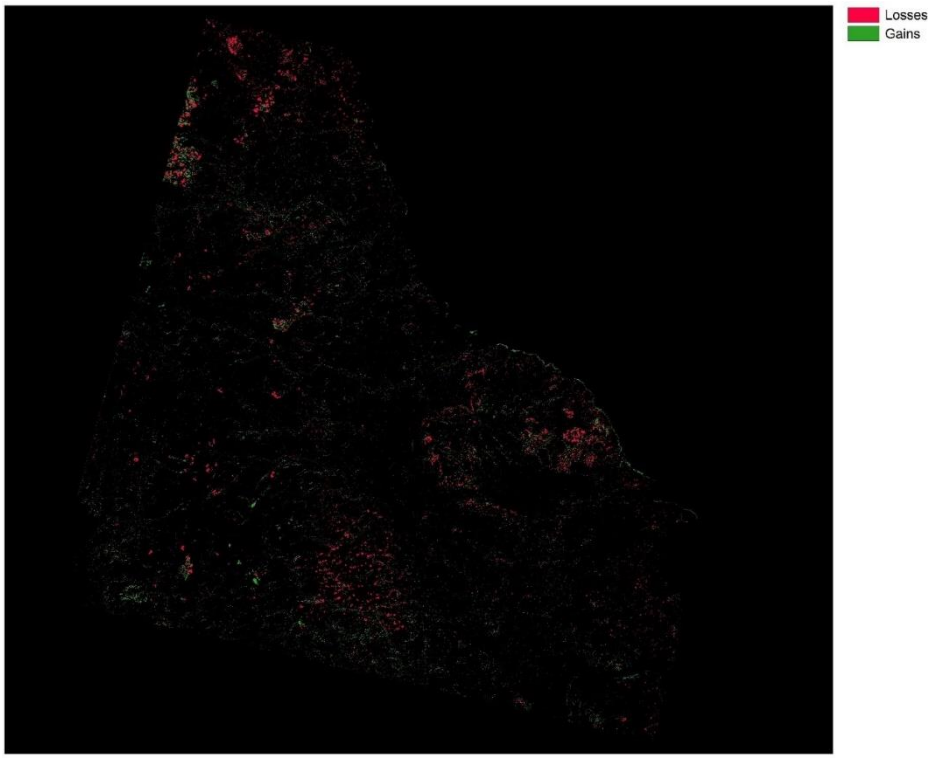

Figure 8: Change map displaying locations of woodland gains and losses between 2004 and 2011. Created using Terrset.

iv. Accuracy Assessment - Error Matrix

The accuracy assessment matrix displays the validation results. Matrix columns show the land cover class of the ground truth pixels, whilst the rows display which class the pixels have been assigned in the image. The diagonal shows the correctly classified pixels. Therefore, incorrectly assigned pixels falling outside the diagonal indicate confusion between the different LCC classes in the validation (Rwanga & Ndambuki, 2017).

In 2004, overall accuracy was 95%, and woodland scored 100% accuracy in both Errors of Commission and Omission. In 2011, overall accuracy was 92%, and woodland scored 80% in Errors of Omission and 100% in Errors of Commission (Table 5). There were two instances where a pixel was classified as woodland but was in fact cloud. However, desktop research indicates woodland was the correct land cover class beneath the cloud.

Overall high percentage and minor range in accuracy indicates minimal confusion between the land cover classes. Water is well classified, with no errors on either accuracy assessment for 2004 or 2011, which is typical given water's unique spectral signature in comparison to other land cover classes. User errors are evident in the agricultural and artificial surface classes. In 2004, the image classification assigned one of the cloud validation pixels as an artificial surface. This aligns with the spectral signature charts that suggested there was some confusion between the artificial surfaces and cloud LCC classes, particularly in 2004. Furthermore, in 2011 there were two instances where pixels that were truthfully artificial surfaces but were classified as agriculture, raising doubts regarding the decrease in coverage of artificial surfaces between 2004 and 2011. Once more, although lacking in direct relevance to woodland bird species, it remains imperative to account for the precision of every LCC class to evaluate the overall validity of the investigation's accuracy.

The overall Kappa coefficient in 2004 was 0.94 and 0.9 in 2011. These high coefficients are rated as almost perfect. Therefore, the classified images produced in this study would provide reliable information to the WNGO and be suitable for further research.

	1	2	3	4	5	6	Total	ErrorC
1	10	0	0	0	0	0	**10**	**0**
2	0	10	1	0	0	1	**12**	**0.166667**
3	0	0	9	0	0	0	**9**	**0**
4	0	0	0	10	0	0	**10**	**0**
5	0	0	0	0	10	1	**11**	**0.090909**
6	0	0	0	0	0	8	**8**	**0**
Total	**10**	**10**	**10**	**10**	**10**	**10**	**60**	
ErrorO	**0**	**0**	**0.100000**	**0**	**0**	**0.200000**		**0.050000**

	1	2	3	4	5	6	Total	ErrorC
1	10	0	0	0	0	0	**10**	**0**
2	0	10	0	0	2	0	**12**	**0.166667**
3	0	0	10	0	0	0	**10**	**0**
4	0	0	0	8	0	0	**8**	**0**
5	0	0	0	0	7	0	**7**	**0**
6	0	0	0	2	1	10	**13**	**0.230769**
Total	**10**	**10**	**10**	**10**	**10**	**10**	**60**	
ErrorO	**0**	**0**	**0**	**0.200000**	**0.300000**	**0**		**0.083333**

Table 5: Error matrices for 08/09/2004 (top) and 28/09/2011 (bottom). Where ErrorO represents Errors of Omission and ErrorC represents Errors of Commission, expressed as proportions. Created using Terrset.

4. Discussion

This analysis accurately classified woodland in the North of England and will be useful for the WNGO to understand the nature and locations of variations in woodland land cover and project possible future changes (Ioannis & Meliadis, 2011). Furthermore, the results could help a variety of stakeholders, such as government, local authorities, agricultural enterprises, and urban planners.

Future studies would benefit from an increase in the number of LCC classes, creating more specific spectral signatures and likely reducing the occurrence of misclassifications. Furthermore, classifying woodland into multiple classes, such as deciduous and coniferous woodland, may also aid the WNGO. When undertaking change analysis, a finer temporal resolution would be beneficial. Woodland pixels on the fringes of a forest boundary were more vulnerable to being assigned to an incorrect class rather than pixels within the interior, with computational algorithms unable to distinguish more subtle differences at lower resolutions. Newer satellites with more advanced sensors, such as Sentinel-2, now offer higher spatial and spectral resolution imagery that can provide more accurate and detailed land cover information.

Regarding the other LCC classes, although overlaps in spectral signatures may indicate mistakes in the creation of training sites, in some cases it was hard to avoid. Classes, such as agriculture and grassland, and artificial surface and cloud, truly share mutual reflectance patterns in specific bands. Crucially, it is extremely difficult to create a land cover map that is entirely precise and fulfils all requirements (Strahler, et al., 2006). Despite these weaknesses, both classifications perform well with high overall accuracy and kappa coefficient.

High altitude cirrus clouds visible in the 2011 scene affected the classification outcome. Clouds can obstruct satellite imagery, making it difficult to accurately classify certain areas. Although from the same year, the reference data and Landsat imagery were taken at different times and therefore brought inconsistencies with cloud coverage, resulting in errors in the accuracy assessment. Furthermore, the angle at which the sun hits the Earth can also affect satellite imagery. Moreover, the presence of shadows cast by buildings, trees, and clouds can affect the spectral signature of a pixel. Consequently, future studies on behalf of the WNGO may benefit from image pre-processing. Conducting atmospheric and geometric correction of the downloaded images reduces the effect of atmospheric haze, shadows, and distortions caused by topography (Phiri, et al., 2018). Given the difficulties creating a highly accurate land cover map of a diverse area based solely on spectral information, future studies may wish to incorporate other ancillary information, such as slope, aspect and elevation and create a decision tree. Additionally, some previous studies divide the areas of interest into ecoregions, or bioregions, and then classify the imagery, which often improves the land cover map and results in less confusion (NASA, 2017).

The findings suggest artificial surfaces decreased between 2004 and 2011. Given urban areas are largely made up of artificial surfaces, the results are contra to typical findings associated with suburban expansion in England (Lawton, et al., 2021). Equally, urban areas tend to be spectrally heterogeneous and often difficult to classify (NASA, 2017). Ideally, a prolonged temporal separation between the scrutinised images would be desirable. Nevertheless, adopting a 7-year interval represents a compromise stemming from the necessity of working with low cloud cover imagery. Ongoing analysis would benefit from using more recent imagery and completion of land change analysis over a longer period. Even though both images are from September, the 2011 image was taken 20 days later in the month. Images from later in the summer, thus later stages of the UK harvest, may see an increase in spectral similarity between bare soils and impervious surfaces (Ioannis & Meliadis, 2011). This may in part explain the reduction in artificial surface coverage between 2004 and 2011, with agricultural pixels having a broader spectral signature in conjunction with the latter stages of the UK harvest.

Although the accuracy assessment results were strong, there were instances of misclassification. Additionally, sampling methods and the number of validation points may have limited the reliability of the results. Any future analysis would likely benefit from more validation points to identify the potential causes of misclassification. Applying a confidence level of 99% rather than 95% to the Fitzpatrick-Lins formula would also be recommended.

5. Conclusion

Overall, the use of advanced image processing algorithms allowed accurate classification of different land cover types with a high degree of precision. The results of this analysis can help inform the WNGO, gaining a deeper understanding of woodland environments to make more informed decisions through time.

6. Figures

7. Tables

8. References

Abburu, S. & Golla, S., 2015. Satellite Image Classification Methods and Techniques: A Review. *International Journal of Computer Applications,* 119(8).

ESRI, 2011. *Environmental Systems Research Institute - Raster Image Processing Tips and Tricks.* [Online] Available at: https://www.esri.com/arcgis-blog/products/spatial-analyst/analytics/raster-image-processing-tips-and-tricks-part-4-image-classification/?rmedium=blogs_esri_com&rsource=/esri/arcgis/2011/01/10/georef4/ [Accessed 10 March 2023].

Fichera, C., Modica, G. & Pollino, M., 2012. Land Cover Classification and Change-detection Analysis using Multi-temporal Remote Sensed Imagery and Landscape Metrics. *European Journal of Remote Sensing,* 45(1), pp. 1-18.

Fitzpatrick-Lins, K., 1981. Comparison of Sampling Procedures and Data Analysis for a Land-use and Land-cover Map. *Photogrammetric Engineering and Remote Sensing,* 47(3), pp. 343-351.

Ioannis, M. & Meliadis, M., 2011. Multi-temporal Landsat Image Classification and Change Analysis of Land Cover/Use in the Prefecture of Thessaloiniki, Greece. *Proceedings of the International Academy of Ecology and Environmental Sciences,* 1(1), p. 15.

Jensen, J., 2015. *Introductory Digital Image Processing.* 4th ed. South Carolina: Pearson.

Karlsson, A., 2003. *Classification of High-resolution Satellite Images.* [Online]
Available at: https://infoscience.epfl.ch/record/63248/files/TPD_
[Accessed 10 March 2023].

Lawton, M., Martí-Cardona, B. & Hagen-Zanker, A., 2021. Urban Growth Derived from Landsat Time Series Using Harmonic Analysis: A Case Study in South England with High Levels of Cloud Cover. *Remote Sensing,* 13(16), p. 3339.

Lillesand, T., Kiefer, R. & Chipman, J., 2015. *Remote Sensing and Image Interpretation..* 7th ed. s.l.:John Wiley & Sons.

NASA, 2017. *National Aeronautics and Space Administration - ARSET Advanced Land Cover Classification Webinar Series.* [Online]
Available at: https://appliedsciences.nasa.gov/sites/default/files/supervised_exercise2_final.pdf
[Accessed 03 March 2023].

ONS, 2022. *Office for National Statistics - Woodland Natural Capital Accounts: 2022.* [Online]
Available at:
https://www.ons.gov.uk/economy/environmentalaccounts/bulletins/woodlandnaturalcapitalaccountsuk/2022
[Accessed 10 March 2023].

Papp, J., 2018. *Quality Management in the Imaging Sciences.* 6th ed. s.l.:Elsevier Health Sciences.

Phalke, A. et al., 2020. Mapping Croplands of Europe, Middle East, Russia, and Central Asia using Landsat, Random Forest, and Google Earth Engine. *ISPRS Journal of Photogrammetry and Remote Sensing,* Issue 167, pp. 104-122.

Phiri, D., Morgenroth, J., Xu, C. & and Hermosilla, T., 2018. Effects of Pre-processing Methods on Landsat OLI-8 Land Cover Classification Using OBIA and Random Forests Classifier. *International Journal of Applied Earth Observation and Geoinformation,* Volume 73, pp. 170-178.

Richards, J. & Jia, X., 2006. Image Classification Methodologies. *Remote Sensing Digital Image Analysis: An Introduction,* pp. 295-332.

Rocchio, L. & Barsi, J., 2016. *National Aeronautics and Space Administration - Technical Details.* [Online]
Available at: https://landsat.gsfc.nasa.gov/about/technical-details/
[Accessed 10 March 2023].

RSPB, 2017. *The Royal Society for the Protection of Birds - Landscape Effects on Woodland Birds.* [Online]
Available at: https://www.rspb.org.uk/our-work/conservation/projects/landscape-effects-on-woodland-birds
[Accessed 10 March 2023].

Rwanga, S. & Ndambuki, J., 2017. Accuracy Assessment of Land Use/Land Cover Classification using Remote Sensing and GIS. *International Journal of Geosciences,* 8(4), p. 611.

Strahler, A. et al., 2006. Global Land Cover Validation: Recommendations for Evaluation and Accuracy Assessment of Global Land Cover Maps. *European Communities, Luxembourg,* 51(4), pp. 1-60.

TerrSet, 2016. *Terrset Manual.* [Online]
Available at: https://clarklabs.org/wp-content/uploads/2016/10/Terrset-Manual.pdf
[Accessed 10 March 2021].

UBC, 2018. *University of British Columbia - Introduction to Image Analysis: Supervised Image Classification.* [Online]
Available at: https://ibis.geog.ubc.ca/courses/geob373/labs/lab5supervised.html
[Accessed 10 March 2023].

USGS, 2023. *U.S. Geological Survey - Earth Explorer.* [Online]
Available at: https://earthexplorer.usgs.gov/
[Accessed 10 March 2023].

Williams, D., Goward, S. & Arvidson, T., 2006. Landsat: Yesterday, today, and tomorrow. Photogrammetric Engineering and Remote Sensing. 72(10), p. 1171.